$\mathbb{Z}_2$-EQUIVARIANT ANALYTIC FOLIATIONS

WALDO ARRIAGADA and PIOTR SKRZYPACZ

Communicated by Liviu Ornea

In these notes, we introduce a geometric characterization of the $\mathbb{Z}_2$-equivariance of the phase space of a complex generic real analytic family with an elliptic equilibrium. The equivariance allows us to understand the interaction between complex and real foliations in terms of an antiholomorphic involution or real structure. The existence of the latter provides an explanation to some rigid phenomena observed in the complex phase portrait (*e.g.* the appearance of complex singularities in the real phase space; the presence of conformal symmetries affecting the invariant of analytic classification; etc.) In the complex phase space the equivariance is called the *real character*. It plays a fundamental role in the characterization of the conformal structure of elliptic equilibria of analytic families of vector fields.

AMS 2010 Subject Classification: 34M35, 34M45, 34C14, 34C23.

Key words: equivariance, Hopf bifurcation, weak focus, blow-up, holonomy.

1. INTRODUCTION

Let M and N be complex manifolds. A differentiable function $\sigma : M \to N$ is called *antiholomorphic* if in terms of a local coordinate z it takes the form $z \mapsto \eta(\overline{z})$ where η is holomorphic and $z \mapsto \overline{z}$ is the standard complex conjugation. By an *antiholomorphic involution* or *real structure* of the complex manifold M we mean an antiholomorphic map $\sigma : M \to M$ such that $\sigma \circ \sigma = id_M$.

Not every pair (M, σ) can be obtained by *complexifying* a real analytic manifold. Indeed, M might not have enough *real points* (fixed points of σ), and in fact it might not have any at all [11]. General and particular properties of real structures on manifolds have been extensively reported in the literature. For example, a detailed study of antiholomorphic involutions of analytic families of abelian varieties can be found in [1].

In these notes, we consider the simplest case where the manifold M is the product $\mathbb{C}^2$. In this case, the fixed point set for any real structure fixing the origin is a totally real 2-plane containing the origin [9]. (A 2-plane in $\mathbb{C}^2$ is totally real if any basis over $\mathbb{R}$ for the plane is also linearly independent over $\mathbb{C}$). Further, let $Z = (\mathbf{z}, \mathbf{w})$ be the standard coordinates of $\mathbb{C}^2$. It is proved [13] that any antiholomorphic involution σ fixing the origin in $\mathbb{C}^2$ has the form

$$\sigma : Z \mapsto P\overline{Z}^T + \beta(\overline{Z}), \tag{1.1}$$

where P is a unitary matrix, and the higher-order terms β satisfy $\beta(\overline{\sigma(Z)}) = -P\overline{\beta}(Z)$. (The bar on β indicates complex conjugation only of the coefficients in the series β). Real maps and vector fields, invariant under the involution, can be defined: a germ of map $f : (\mathbb{C}^2, 0) \to (\mathbb{C}, 0)$ is called σ-real if it is a conjugacy between σ and the standard complex conjugation. A germ of complex map f or complex vector field $\mathbf{F}$, with $f, \mathbf{F} : (\mathbb{C}^2, 0) \to (\mathbb{C}^2, 0)$ is called σ-real if it commutes with the involution (1.1).

By definition the fixed points of σ (i.e. the solutions of the system $Z = \sigma(Z)$) satisfy, in terms of the chart $(\mathbf{z}, \mathbf{w})$, the equation $\mathbf{w} = p\overline{\mathbf{z}} + q\overline{\mathbf{w}} + \cdots$, with $p \neq 0$. A simple transformation allows us to assume $q = 0$, so that the system is equivalent to a single equation $\mathbf{w} = p\overline{\mathbf{z}} + \gamma(\mathbf{z}, \overline{\mathbf{z}})$, where $\gamma = \mathcal{O}(|\mathbf{z}|^2)$. We introduce coordinates (z, w) by $\mathbf{w} = pw + \gamma(z, w)$, and $\mathbf{z} = z$. This chart brings (1.1) into the antiholomorphic involution $(z, w) \mapsto (\overline{z}, \overline{w})$. Finally, the change $(z, w) \mapsto (z + \mathrm{i}w, z - \mathrm{i}w)$ transforms the latter involution into

$$(z, w) \mapsto (\overline{w}, \overline{z}). \tag{1.2}$$

Hence, in $\mathbb{C}^2$ it suffices to consider the standard particular case (1.2) corresponding to $P = \left(\begin{smallmatrix} 0 & 1 \\ 1 & 0 \end{smallmatrix}\right)$ and $\beta \equiv 0$. The fixed point set of this involution coincides with the totally real plane $\mathbb{R}^2 = \{w = \overline{z}\}$.

If $\mathbf{F}$ is an autonomous and σ-real (in the sense of the standard antiholomorphic involution (1.2)) germ of a complex analytic vector field in $(\mathbb{C}^2, 0)$, then its linear part has the form

$$(az + bw)\frac{\partial}{\partial z} + (\overline{b}z + \overline{a}w)\frac{\partial}{\partial w}, \tag{1.3}$$

where $a, b \in \mathbb{C}$. If $b \equiv 0$, the system is called *elliptic* or *monodromic* [8, 15] provided $\mathrm{Re}(a) = 0$ but $\mathrm{Im}(a) \neq 0$. Evidently, the eigenvalues of the linear part are complex conjugate.

Let η denote a tuple of one or more complex parameters defined on a polydisk containing zero and of small diameter. Any family of vector fields $\mathbf{F}_\eta$ which depends analytically on the parameters is called either an elliptic *family, deformation* or *unfolding* of the single vector field $\mathbf{F}$, if $\mathbf{F}_0 \equiv \mathbf{F}$. We say that the unfolding $\mathbf{F}_\eta$ is σ-real if (1.2) is a conjugacy between $\mathbf{F}_\eta$ and the parameter-conjugate vector field $\mathbf{F}_{\overline{\eta}}$. Elliptic unfoldings are called *generic* provided the real part of the complex-conjugate eigenvalues crosses the imaginary axis at non-zero speed,

$$\frac{\mathrm{d}}{\mathrm{d}\eta}\mathrm{Re}(a(\eta))|_{\eta=0} \neq 0.$$

Generic elliptic germs of analytic vector fields form an important class in the theory of holomorphic singular foliations [2, 8]. For example, for certain values of the unfolding parameter the Hopf bifurcation takes place, provided the system does not unfold a center on those values. In this case, the local geometry of the phase portrait around the equilibria allows us to study, among other properties, the *temporal* behavior of the solution curves [3, 5, 6]. The most remarkable property is that elliptic equilibria of planar analytic germs of vector fields are *intrinsically real.* This means that the complex foliation can be *realified* in the sense of (1.2). In any case, the complex foliation itself is the complexification of an underlying real analytic foliation (see next section) lying on a totally real 2-plane embedded in $\mathbb{C}^2$. Conversely, the standard complexification of a real analytic elliptic foliation is invariant under (1.2). This provides a complete characterization of the conformal symmetries associated with the complex equilibrium. In article [3] we have described the conformal symmetries affecting the invariant (or modulus) of the analytic classification of the singularity. These symmetries are generalized complex reflections around a *real* axis in the orbit space of the *Poincaré monodromy.* However, these symmetries can occur when the parameter belongs to open symmetric sectorial domains $V_\pm$ around the real axis. In this case, the parameter belongs to the Poincaré domain. If the values of the parameter are taken in open sectorial domains covering both $V_\pm$ and the imaginary axis then the parameter belongs to the Siegel domain. A description of the dynamics in the intersection of Poincaré and Siegel domains of the parameter space can be found in [4].

2. $\mathbb{Z}_2$-EQUIVARIANCE

Let n be a positive integer, and let G be a (compact) group which can be represented in $\mathbb{R}^n$ by matrices $\{T_g\}$:

$$T_e = I_n, \quad T_{g_1 g_2} = T_{g_1} T_{g_2},$$

for any $g_1, g_2 \in G$. The element $e \in G$ is the group unit ($eg = ge = g$), and I_n is the $n \times n$ unit matrix. Consider an analytic germ of differential equations

$$\frac{\mathrm{d}\vec{x}}{\mathrm{d}t} = F_\eta(\vec{x}), \quad \vec{x} \in \mathbb{R}^n$$

depending analytically on a multiparameter $\eta \in \mathbb{R}^k$. This family is called *invariant* with respect to the representation $\{T_g\}$ of the group G, or simply G-equivariant, if

$$T_g \cdot F_\eta = F_\eta \cdot T_g,$$

for all $g \in G$, where the dot represents the action of G on the vector field F_η.

In these terms, the real structure (1.2) corresponds in $\mathbb{R}^4$ to the linear transformation T_σ represented by the premultiplication by the matrix

$$M = \begin{bmatrix} 0 & 0 & 1 & 0 \\ 0 & 0 & 0 & -1 \\ 1 & 0 & 0 & 0 \\ 0 & -1 & 0 & 0 \end{bmatrix}.$$

That is, if $\vec{X} = (x_1, y_1, x_2, y_2)$ are the standard coordinates of $\mathbb{R}^4$, then the antiholomorphic involution (1.2) in $\mathbb{C}^2$ corresponds to the linear transformation

$$T_\sigma : \begin{pmatrix} x_1 \\ y_1 \\ x_2 \\ y_2 \end{pmatrix} \mapsto \begin{pmatrix} x_2 \\ -y_2 \\ x_1 \\ -y_1 \end{pmatrix}$$

in $\mathbb{R}^4$ for the complex coordinates $z = x_1 + \mathrm{i}y_1$ and $w = x_2 + \mathrm{i}y_2$. Inasmuch as $M^2 = I_4$, the transformation T_σ is an involution, $T_\sigma^{\circ 2} = T_e$, where T_e is the *identity* linear transformation, represented by premultiplication by the identity matrix I_4. This representation decomposes $\mathbb{R}^4$ into a direct sum

$$\mathbb{R}^4 = \Sigma^+ \oplus \Sigma^-,$$

where $\Sigma^+ = \{\vec{X} \in \mathbb{R}^4 : M\vec{X} = \vec{X}\}$ and $\Sigma^- = \{\vec{X} \in \mathbb{R}^4 : M\vec{X} = -\vec{X}\}$.

The subspace Σ^+ is the fixed point subspace of the transformation T_σ. In the complex representation (1.2), the space Σ^+ itself corresponds to $\{z = \overline{w}\}$ which is canonically identified with the real plane $\mathbb{R}^2 \subset \mathbb{C}^2$. The space Σ^+ will be called *the real plane.*

On the other hand, in terms of the complex coordinates z, w the subspace Σ^- is the set of fixed points of $-\sigma$. That is, it corresponds to $\{z = -\overline{w}\}$. By analogy, the space Σ^- will be called *the imaginary plane* (in the sense of the direct sum above).

In the sequel, we will assume that $\eta \in \mathbb{R}$. (The case $\eta \in \mathbb{R}^k$ presents some substantial differences). Let $\mathbf{F}_\eta$ denote the germ of a generic analytic unfolding of an elliptic vector field with the linear part (1.3) and which depends analytically on the parameter. Since $\mathbf{F}_\eta$ commutes with the involution σ on real values of the parameter, this vector field is essentially real. In other words, the flow of $\mathbf{F}_\eta$ leaves the real plane invariant. Therefore, the complex foliation defined by the system induces a real foliation on Σ^+. Such a real foliation must hence be the phase portrait of a planar real analytic vector field F_η on Σ^+. The vector field F_η is called the *realification* of $\mathbf{F}_\eta$ [7]. Therefore, if we denote $G = \{T_e, T_\sigma\} \sim \mathbb{Z}_2$, then parameter-dependent vector field $\mathbf{F}_\eta$ is $\mathbb{Z}_2$-equivariant for real values of the parameter:

$$M\mathbf{F}_\eta(\vec{X}) = \mathbf{F}_\eta(M\vec{X}), \quad \vec{X} \in \mathbb{R}^4, \ \eta \in \mathbb{R}. \tag{2.1}$$

Moreover, division by $\mathrm{Im}(a)$ (for the constant a in (1.3)) and subsequent time scaling $t \mapsto \mathrm{Im}(a)t$ allows us to take $\varepsilon = \mathrm{Re}(a)/\mathrm{Im}(a)$ as a new parameter. This new parameter is an invariant under analytic changes of coordinates [2].

These considerations prove that generic σ-invariant germs of analytic vector fields in $(\mathbb{C}^2, 0)$ have the standard form

$$\begin{aligned} \frac{\mathrm{d}z}{\mathrm{d}t} &= (\varepsilon + \mathrm{i})z + \sum_{j+k\geq 2} a_{jk}(\varepsilon) z^j w^k, \\ \frac{\mathrm{d}w}{\mathrm{d}t} &= (\varepsilon - \mathrm{i})w + \sum_{j+k\geq 2} \overline{a_{jk}(\overline{\varepsilon})} z^k w^j, \end{aligned} \tag{2.2}$$

where the coefficients a_{jk} depend analytically on ε. These unfoldings are (non-exhaustive) generic unfolding of $1:1$ resonant complex saddle points in $\mathbb{C}^2$, with the ratio of eigenvalues equal to -1, see [12]. The $\mathbb{Z}_2$-equivariance (2.1) of $\mathbf{F}_\eta$ is called the *real character* of this system. Let (x, y) be the real coordinates of Σ^+. The real foliation induced on this surface by (2.2) is defined by the integral curves of a real system of the form

$$\begin{aligned} \frac{\mathrm{d}x}{\mathrm{d}t} &= \varepsilon\, x - y + \sum_{j+k\geq 2} b_{jk}(\varepsilon) x^j y^k, \\ \frac{\mathrm{d}y}{\mathrm{d}t} &= x + \varepsilon\, y + \sum_{j+k\geq 2} c_{jk}(\varepsilon) x^j y^k, \end{aligned} \tag{2.3}$$

where the b_{jk}'s and c_{jk}'s depend analytically on the parameter ε. The first Lyapunov constant can be explicitly computed in terms of the coefficients of the vector field:

$$\ell_1 = 3b_{30} + b_{12} + c_{21} + 3c_{03} + \frac{1}{\beta}\Big(b_{11}(b_{20}+b_{02}) - c_{11}(c_{20}+c_{02}) - 2b_{20}c_{20} + 2b_{02}c_{02}\Big).$$

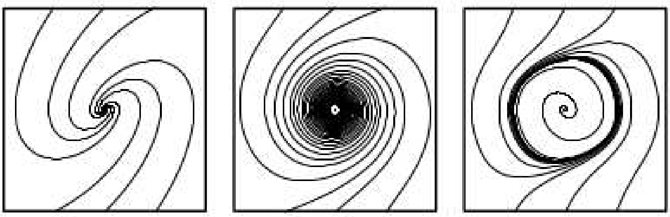

(a) Strong focus (b) Weak focus (c) Limit cycle

Fig. 1 – The supercritical Hopf bifurcation of order 1.

It is known that if $\ell_1(0) \neq 0$ then the system exhibits a generic Hopf bifurcation: the generic coalescence of a focus with a limit cycle [10]. The geometric configuration of the phase space at the bifurcation value is denominated a weak focus. Weakness means that the convergence of integral curves to the origin is slower than that of logarithmic spirals of strong foci. The Hopf bifurcation is *subcritical* if the cycle is present on negative values of ε. It is *supercritical* otherwise. Whether a Hopf bifurcation is subcritical or supercritical can be found from the sign of the first Lyapunov coefficient. Positive sign of $\ell_1(0)$ indicates a subcritical Hopf bifurcation and negative sign of $\ell_1(0)$ corresponds to a supercritical Hopf bifurcation, see Fig. 1.

Definition 2.1. The sign of $\ell_1(0)$ is called the sign of the system.

In the next sections, we will study the relationship between complex and real singular holomorphic foliations of this family. This connection is only fully appreciated in the blow-up space.

3. COMPLEX AND REAL BLOW-UP

Let $\mathbb{P}^1$ denote the projective space (Riemann sphere) and define the quasi-projective variety

$$\mathbb{M} = \{([t_2 : t_1], (z, w)) \in \mathbb{P}^1 \times \mathbb{C}^2 : zt_1 - wt_2 = 0\}, \tag{3.1}$$

where $[t_2 : t_1]$ is the line at infinity through (t_2, t_1) (homogeneous coordinates on $\mathbb{P}^1$). Projection onto $\mathbb{C}^2$ induces a surjective morphism $\varrho : \mathbb{M} \to \mathbb{C}^2$, with

$$\varrho^{-1}(z, w) = \begin{cases} \mathbb{P}^1 \times \{0\}, & (z, w) = (0, 0), \\ ([z : w], (z, w)), & (z, w) \neq (0, 0). \end{cases}$$

The fiber $S = \varrho^{-1}(0, 0)$ is a projective line, called the *exceptional line.* Away from zero ϱ^{-1} gives an isomorphism between $\mathbb{C}^2\backslash\{0\}$ and $\mathbb{M}\backslash S$. The map ϱ is called the *(standard) monoidal map.* The analytic curve $S \subset \mathbb{M}$ is called *(standard) exceptional divisor.* The pair $(\varrho, \mathbb{M})$ is the *blow-up* of $\mathbb{C}^2$ at zero.

By definition, the surface $\mathbb{M}$ is embedded in the complex 3-dimensional space $\mathbb{P}^1 \times \mathbb{C}^2$. It carries the compact curve (Riemann sphere) $\mathbb{P}^1 \times \{0\} = S$ on it. The points of S correspond to the lines through the origin in $\mathbb{C}^2$, see Fig. 5.

The standard affine covering $\mathbb{P}^1 = U_1 \cup U_2$, where $U_1 = \{[t_2 : t_1] : t_1 \neq 0\}$ and $U_2 = \{[t_2 : t_1] : t_2 \neq 0\}$, induces a covering $\mathbb{M} = V_1 \cup V_2$, with

$$V_1 = \left\{ t_1 \neq 0,\ z - w\frac{t_2}{t_1} = 0 \right\},$$
$$V_2 = \left\{ t_2 \neq 0,\ z\frac{t_1}{t_2} - w = 0 \right\}.$$

By using coordinates $(Z, w) = (\frac{t_2}{t_1}, w)$ for V_1, and $(W, z) = (\frac{t_1}{t_2}, z)$ for V_2, we see that V_1 and V_2 are both isomorphic to $\mathbb{C}^2$. The transition map between these charts is a monomial transformation $\varphi : V_1 \to V_2$,

$$\varphi(Z, w) = \left(\frac{1}{Z}, Zw\right) = (W, z) \tag{3.2}$$

with inverse $\varphi^{-1}(W, z) = (\frac{1}{W}, Wz)$, and hence $\varphi^{\circ 2} = id$. Thus $\mathbb{M}$ is indeed a nonsingular 2-dimensional complex analytic manifold. Observe that the map $\varrho : \mathbb{M} \to \mathbb{C}^2$ in these charts is polynomial, hence globally holomorphic:

$$\varrho|_{V_1} = c_1, \quad \varrho|_{V_2} = c_2,$$

where

$$c_1 : (Z, w) \mapsto (Zw, w) \text{ and } c_2 : (W, z) \mapsto (z, zW). \tag{3.3}$$

Let $\mathcal{F}_\varepsilon$ be the singular foliation of the system (2.2). The blow-up of $\mathcal{F}_\varepsilon$ is the singular holomorphic foliation

$$\widetilde{\mathcal{F}}_\varepsilon = \varrho^* \mathcal{F}_\varepsilon \tag{3.4}$$

extending the preimage foliation $\varrho^{-1}(\mathcal{F}_\varepsilon)$ of the surface $\mathbb{M} \backslash S$. One may have a priori two possibilities for the blown-up foliation $\widetilde{\mathcal{F}}_\varepsilon$: either different points of S belong to different leaves of $\widetilde{\mathcal{F}}_\varepsilon$, or the exceptional divisor S is a separatrix of $\widetilde{\mathcal{F}}_\varepsilon$. In the former case leaves of this foliation cross S transversally at all points, eventually except for finitely many tangency points. On the other hand, a singular point of $\mathcal{F}_\varepsilon$ is called *non-dicritical* if the latter case holds; that is, the exceptional divisor S is a separatrix of $\varrho^* \mathcal{F}_\varepsilon$. Otherwise the singular point is called dicritical. The use of a real atlas in the blow-up space allows us to solve the dichotomy.

3.1. **The realified atlas**

Notice that S in complex charts (Z, w) and (W, z) is determined by

$$S \cap V_1 = \{z = 0\}, \quad S \cap V_2 = \{w = 0\}.$$

As the two sets are isomorphic to $\mathbb{C}$, they can be *realified.* Indeed, the real projective line $\mathbb{R}P^1$ is a closed loop on the Riemann sphere $\mathbb{P}^1$ which is visible as the real line $\mathbb{R}$ in the affine charts $S \cap V_1$ and $S \cap V_2$. This can be proved as follows. The complex Möbius strip $\mathbb{M}$ intersects the real variety $\mathbb{R}P^1 \times \mathbb{R}^2$ at $\{t_1 = \overline{t_2}\}$ and $\{z = \overline{w}\}$. This intersection is a real Möbius strip:

$$\mathfrak{M} = \{([a : b], (x, y)) \in \mathbb{R}P^1 \times \mathbb{R}^2 : xb + ya = 0\},$$

where $z = x + \mathrm{i}y$ and $t_1 = a + \mathrm{i}b$. Such a surface can be explicitly parametrized in real charts.

PROPOSITION 3.1. *The covering* $\mathbb{M} = V_1 \cup V_2$ *induces a real covering* $\mathfrak{M} = \mathfrak{V}_1 \cup \mathfrak{V}_2$, *where* $\mathfrak{V}_1$, $\mathfrak{V}_2$ *are both isomorphic to* $\mathbb{R}^2$.

Proof. The charts V_1, V_2 intersect $\mathbb{R}P^1 \times \mathbb{R}^2$ at $t_2 = \overline{t_1}$ and $w = \overline{z}$. Then,

$$\begin{aligned} V_1 \cap \left(\{t_2 = \overline{t_1}\} \times \{w = \overline{z}\}\right) &= \{t_1 \neq 0,\, zt_1 - \overline{zt_1} = 0\} \\ &= \{t_1 \neq 0,\, \mathrm{Im}(zt_1) = 0\} \\ &= \{(a,b) \neq (0,0),\, xb + ya = 0\} \subset \mathbb{R}P^1 \times \mathbb{R}^2, \end{aligned}$$

where $z = x + \mathrm{i}y$ and $t_1 = a + \mathrm{i}b$ with $x, y, a, b \in \mathbb{R}$. If $a \neq 0$ the chart

$$\mathfrak{V}_1 = \left\{([a:b],(x,y)) \in \mathbb{R}P^1 \times \mathbb{R}^2 : a \neq 0,\, x\frac{b}{a} + y = 0\right\} \sim \mathbb{R}^2$$

is parametrized by $(x,u) \in \mathbb{R}^2$, where $u = -\frac{b}{a}$. If $b \neq 0$, the chart

$$\mathfrak{V}_2 = \left\{([a:b],(x,y)) \in \mathbb{R}P^1 \times \mathbb{R}^2 : b \neq 0,\, x + y\frac{a}{b} = 0\right\} \sim \mathbb{R}^2$$

is parametrized by $(v,y) \in \mathbb{R}^2$, where $v = -\frac{a}{b}$. $\square$

The monoidal map $\varrho : \mathbb{M} \to \mathbb{C}^2$ induces a real map (denoted by ϱ again) between $\mathfrak{M}$ and $\mathbb{R}^2$, $\varrho|_{\mathfrak{V}_1} = r_1$, and $\varrho|_{\mathfrak{V}_2} = r_2$, where

$$r_1 : (x,u) \mapsto (x, xu) \text{ and } r_2 : (v,y) \mapsto (vy, y). \tag{3.5}$$

Hence, the exceptional divisor $S = \mathbb{P}^1 \times \{0\} \subset \mathbb{P}^1 \times \mathbb{C}^2$ intersects $\mathbb{R}P^1 \times \mathbb{R}^2$ at $\mathbb{R}P^1 \times \{0\} \simeq \mathbb{S}^1$, which is the equator of the real Möbius strip $\mathfrak{M}$, see Fig. 2. The equator is then covered by real charts $\mathbb{S}^1 \cap \mathfrak{V}_1 = \{x = 0\}$ and $\mathbb{S}^1 \cap \mathfrak{V}_2 = \{y = 0\}$.

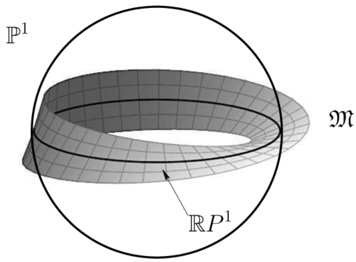

Fig. 2 – The real line (equator) of the exceptional divisor.

3.2. **The tangent polynomial of the unfolding.**

Let $F_\varepsilon(x,y)$ be the germ of a real analytic parameter-dependent vector field with the linear part

$$A_\varepsilon(x,y)\frac{\partial}{\partial x} + B_\varepsilon(x,y)\frac{\partial}{\partial y},$$

having an isolated singularity of order 1. (This means that the coefficients $A_\varepsilon, B_\varepsilon$ are homogeneous polynomials of degree 1 and at least one of these two homogeneous polynomials does not vanish identically). The singular point of the vector field is called *generalized elliptic* [8] if the real homogeneous degree-2 polynomial $p_\varepsilon = xB_\varepsilon - yA_\varepsilon \in \mathbb{R}[x,y]$ is non-vanishing except at zero. The polynomial p_ε is called *the tangent polynomial* of the vector field. The singular points on the exceptional divisor after real blow-up, are roots of the polynomial

$$x^{-2}p_\varepsilon(x,xu) = B_\varepsilon(1,u) - uA_\varepsilon(1,u),$$

where u is defined in (3.5). For a generalized elliptic singularity this polynomial is not identically zero and then the blow-up is always non-dicritical. It is easy to see then that there are no singular points on the real equator $\mathbb{R}P^1 \subset S$ in the chart (x,u). Similarly, the point $u = \infty$ (mapped as $v = 0$ in the second chart) is also non-singular.

As an immediate consequence, a real analytic singularity is generalized elliptic if and only if it is non-dicritical and after the blow-up it has no singularities on the real projective line $\mathbb{R}P^1 \subset \mathbb{P}^1$ of the exceptional divisor. In coordinates this means the following.

PROPOSITION 3.2. *The foliation of* (2.3) *has two singular points at* $(x,u) = (0,\mathrm{i})$ *and* $(x,u) = (0,-\mathrm{i})$ *in the first chart of the real blow-up* (3.5). *These singularities are, therefore, complex and they are located at* $(Z,w) = (0,0)$ *and* $(Z,w) = (\infty,0)$ *respectively, in the first complex chart of the blow-up. Further, system* (2.3) *is generalized elliptic and the points* $(x,u) = (0,0)$ *and* $(x,u) = (0,\infty)$ *on the equator* $\mathbb{R}P^1 \subset \mathbb{P}^1$ *are non singular.*

Proof. The tangent polynomial is

$$p_\varepsilon(x,y) = x(x+\varepsilon\, y) - y(\varepsilon\, x - y) = x^2 + y^2,$$

which is non-vanishing except at zero. Its pullback into (x,u) coordinates is $p_\varepsilon(x,xu) = x^2(1+u^2)$ and hence the singular points are complex and they are located at $u = \pm\mathrm{i} \in \mathbb{P}^1$. As these are the only singular points in the complex blow-up, the points $u = 0, \infty$ (mapped as $v = \infty, 0$ in the other chart) are non singular. Taking $u = -\frac{b}{a}$, the real point $(x,u) = (0,0)$ corresponds to $b = 0$ when $t_1 = a + \mathrm{i}b$ in (3.1). This means $Z = \frac{t_2}{t_1} = \frac{a}{a} = 1$. Analogously, the real point $(x,u) = (0,\infty)$ corresponds to $a = 0$ and then $Z = \frac{-\mathrm{i}b}{\mathrm{i}b} = -1$. Therefore the points $Z = -1, 1$ (mapped as $W = -1, 1$ in the second complex chart) are non singular.

On the other hand, the imaginary point $(x,u) = (0,+\mathrm{i})$ corresponds to $b = -\mathrm{i}a$, and then $\mathrm{i}(a - \mathrm{i}b) = 0$. As $t_2 = \overline{t_1} = a - \mathrm{i}b$ in the real coordinates, we get $t_2 = 0$, and hence $Z = 0$. The other point $(x,u) = (0,-\mathrm{i})$ yields $b = \mathrm{i}a$ or $\mathrm{i}(a + \mathrm{i}b) = 0$. That is, $t_1 = 0$ and this is $Z = \infty$. The singular points of the complex chart (V_1, c_1) are therefore located at $(Z,w) = (0,0)$ and $(Z,w) = (\infty,0)$ on the Riemann sphere. $\square$

In particular, the singular points of a weak focus are not detected in the real plane after blow-up, see Fig. 3.

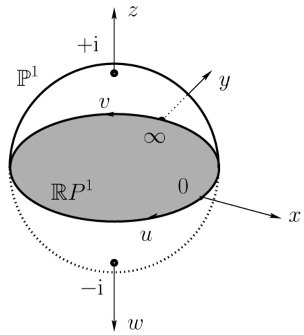

Fig. 3 – The exceptional divisor $S \simeq \mathbb{P}^1$ in real coordinates (x, u).

4. POINCARÉ MONODROMY

Each point of the exceptional divisor S represents a complex line through zero in $\mathbb{C}^2$, see Fig. 5. Since the singular points of the foliation (3.4) are non-dicritical all the lines $\Sigma_\mu : \{z = \mu w\}$ are transversal to $\mathcal{F}_\varepsilon$ provided $\mu \neq 0, \infty$. More precisely, we have the following result.

PROPOSITION 4.1. *The affine collection* $\{\Sigma_\mu\}_\mu$ *is a transverse fibration for the foliation* (2.2) *in a neighborhood of zero.*

Proof. Since $\Sigma_\mu = \{z = \mu w\} = \{\frac{z}{w} = \mu\}$, we use equations (2.2) and get

$$\frac{\mathrm{d}}{\mathrm{d}t}\left(\frac{z}{w}\right) = \frac{\frac{\mathrm{d}z}{\mathrm{d}t}w - z\frac{\mathrm{d}w}{\mathrm{d}t}}{w^2} = \frac{z}{w}(2\mathrm{i} + \cdots) = 2\mathrm{i}\mu + \cdots \neq 0$$

for z, w sufficiently small. $\square$

If $\mu = 1$ we will simply denote Σ the corresponding surface. The structure $\Sigma \cap \Sigma^+ \simeq \mathbb{R}$ is the real line embedded in the real plane. We endow these surfaces with a parametrization by the w coordinate. We will use the same notation for the pullback of Σ_μ in complex charts: $\Sigma_\mu = \{Z = \mu\}$ in the c_1 direction of the complex Möbius strip, and $\Sigma_\mu = \{W = \mu^{-1}\}$ in the c_2 direction of the complex Möbius strip.

In particular, the holonomy map of the family (2.2) along the loop $\mathbb{R}P^1$ in the c_1 direction of the blow-up, is well defined for the cross section Σ with the coordinate w as a local chart on it, see Fig. 4. Inasmuch as (2.2) is analytic, the real singular foliation on the real Möbius strip is well defined. The holonomy map along the circle $\mathbb{R}P^1$ is therefore real analytic. Note, however, that this loop does not belong entirely to any of the two canonical real charts $\mathfrak{V}_1$ and $\mathfrak{V}_2$: to compute the holonomy in the real chart (x, u) one has to *continue* across infinity $u = \infty$ that is, pass to the other chart. This problem can be easily avoided after complexification: if the singularity is generalized elliptic, the holonomy can be computed in the chart (x, u) as the result of analytic continuation along the semi-circular loop

$$[-R, R] \cup \{|u| = R, \mathrm{Im}(u) > 0\}, \quad R > 1$$

which is homotopic to $\mathbb{R}P^1$.

Definition 4.2. The holonomy map $\mathcal{Q}_{1,\varepsilon} : \Sigma \to \Sigma$ of the family (2.2) in the (Z, w) chart of the blow-up is the semi-Poincaré map or semi-monodromy of the system. The standard monodromy $\mathcal{P}_\varepsilon$ of the system is the second iterate $\mathcal{Q}_{1,\varepsilon}^{\circ 2}$. The holonomy map of (2.2) in (W, z) coordinates is denoted by $\mathcal{Q}_{2,\varepsilon} : \Sigma \to \Sigma$.

The complex description of the semi-monodromy immediately allows us to prove its analyticity and that of the monodromy map.

THEOREM 4.3. *The semi-monodromy $\mathcal{Q}_{1,\varepsilon}$ of a generalized elliptic singular point is an orientation reversing (that is, $\mathcal{Q}'_{1,\varepsilon}(0) = -1$) germ of diffeomorphism, which is also real analytic on* $(\mathbb{R}, 0)$, *including the origin.*

The holonomy operator $\mathcal{Q}_{1,\varepsilon}$ of the system (2.2) is visible on the real plane $(\mathbb{R}^2, 0)$ before the blow-up: the cross-section Σ blows-down as the x-axis on the (x, y)-plane. Indeed, the blow-down of Σ is $\{z = w\}$ and since $z = \overline{w}$, we must have $\mathrm{Im}(z) = y = 0$, which is the x-real axis. By construction, $(\mathcal{Q}_{1,\varepsilon}(x), 0)$ is the first point of intersection with the x-axis of a solution starting at $(x, 0)$, after continuation counterclockwise, see Fig. 4.

THEOREM 4.4. *The Poincaré monodromy $\mathcal{P}_\varepsilon : \Sigma \to \Sigma$ of the complex family* (2.2) *is an analytic germ of diffeomorphism which has the form*

$$\mathcal{P}_\varepsilon(w) = \mathrm{e}^{2\pi\,\varepsilon} w \pm \mathrm{e}^{2\pi\,\varepsilon}\big(2\pi + O(\varepsilon)\big) w^3 + O(w^4). \tag{4.1}$$

Proof. The analyticity follows from definition. Write (2.3) in polar coordinates (r, θ) :

$$\begin{cases} \dfrac{\mathrm{d}r}{\mathrm{d}t} = r(\varepsilon + sr^2) + g(r, \theta), \\[2ex] \dfrac{\mathrm{d}\theta}{\mathrm{d}t} = 1 + h(r, \theta), \end{cases} \tag{4.2}$$

where $s = \pm 1$ is the sign of the system, see Definition 2.1. The dependence of the terms $g(r, \theta) = O(|r|^4)$, $h(r, \theta) = O(|r|^3)$ on the parameter ε is not explicitly

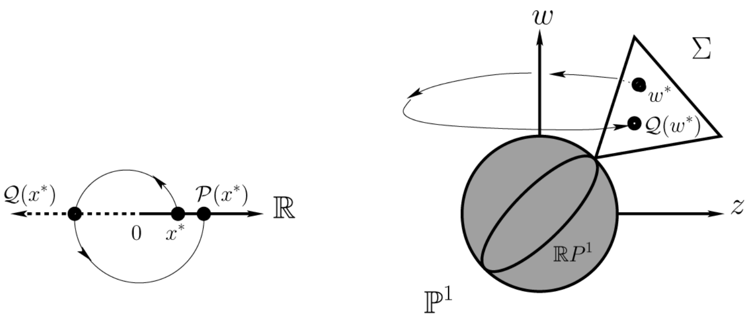

Fig. 4 – The complexification of the holonomy in the blow-up.

mentioned to simplify notations. An orbit of (4.2) starting at $(r, \theta) = (r_0, 0)$ has the following representation: $r = r(\theta, r_0)$, $r_0 = r(0, r_0)$ with r satisfying the equation

$$\frac{\mathrm{d}r}{\mathrm{d}\theta} = \frac{r(\varepsilon + sr^2) + g}{1 + h} = r(\varepsilon + sr^2) + R(r, \theta), \tag{4.3}$$

where $R(r, \theta) = O(|r|^4)$. Notice that the transition from (4.2) to (4.3) is equivalent to the introduction of a new time parametrization in which $\mathrm{d}\theta/\mathrm{d}t = 1$ which implies that the return time to the half-axis $\theta = 0$ is the same for all orbits starting on this axis with $r_0 > 0$. Since $r(\theta, 0) \equiv 0$ we can write the Taylor expansion for $r(\theta, r_0)$,

$$r = u_1(\theta) r_0 + u_2(\theta) r_0^2 + u_3(\theta) r_0^3 + O(|r_0|^4). \tag{4.4}$$

Substituting (4.4) into (4.3) and solving the resulting linear differential equations at corresponding powers of r_0 with initial conditions $u_1(0) = 1$, $u_2(0) = u_3(0) = 0$, yields

$$u_1(\theta) = \mathrm{e}^{\varepsilon \theta}, \quad u_2(\theta) \equiv 0, \quad u_3(\theta) = s\mathrm{e}^{\varepsilon \theta} \left(\frac{\mathrm{e}^{2\varepsilon \theta} - 1}{2\varepsilon} \right).$$

Notice that these expressions are independent of the term $R(r, \theta)$. Therefore, the standard monodromy $r_0 \mapsto r_{\mathcal{P}} = r(2\pi, r_0)$ has the form

$$r_{\mathcal{P}} = \mathrm{e}^{2\pi \varepsilon} r_0 + s\mathrm{e}^{2\pi \varepsilon} \big(2\pi + O(\varepsilon)\big) r_0^3 + O(r_0^4) \tag{4.5}$$

for all $R = O(r_0^4)$. The complexification of (4.5) yields the expression (4.1) in the w coordinate. $\square$

As a consequence, the real germ of the semi-monodromy is simply $r(\pi, r_0)$ in the proof above. Since $\mathcal{P}_\varepsilon = \mathcal{Q}_{1,\varepsilon}^{\circ 2}$, the semi-monodromy has the form

$$\mathcal{Q}_0^{c_1}(w) = -\mathrm{e}^{\pi \varepsilon} w \pm \mathrm{e}^{\pi \varepsilon} \big(\pi + O(\varepsilon)\big) w^3 + o(w^3).$$

Proposition 4.5. *The (complex) Poincaré monodromy $\mathcal{P}_\varepsilon$ sends the real line into itself, provided the parameter be real. In particular, the complex monodromy of the system* (2.2) *is the complexification of the Poincaré first return map of the family* (2.3).

Proof. Let $\varepsilon \in \mathbb{R}$ be given and take an orbit γ of the system (2.2) (for real time) starting at the point $z_0 = w_0 \in \Sigma$ and returning to a point $z_1 = w_1 \in \Sigma$ close to $w_0 : w_1 = \mathcal{P}_\varepsilon(w_0)$. If $z_0 = \overline{w_0}$, the real trajectory of this point coincides with γ (which is then contained in $\mathbb{R}^2$). Hence $z_1 = \overline{w_1}$ because the flow is real for real values of the parameter (that is, the orbits starting at real initial conditions are contained in Σ^+, due to the real character of the family). Therefore,

$$\mathcal{P}_\varepsilon(z_0) = z_1 = \overline{w_1} = \overline{\mathcal{P}_\varepsilon(w_0)} = \overline{\mathcal{P}_\varepsilon(\overline{z_0})}.$$

Since $\mathcal{P}_\varepsilon$ depends analytically on ε the Schwarz reflection principle implies that $\mathcal{P}_\varepsilon$ is a real germ. $\square$

Denote by $f(x,\varepsilon)$ the displacement function $f = \mathcal{P}_\varepsilon - id$ for some choice of a cross-section, say, the semiaxis $\mathbb{R}_+ = \{y = 0, x > 0\}$, and an analytic chart x on this cross-section. By definition, sufficiently small limit cycles of the system (2.2) intersect $\mathbb{R}_+$ at isolated zeros of f. The map (4.1) can easily be analyzed for sufficiently small r_0 and $|\varepsilon|$. For instance, if the sign of the system is $s = -1$, there is a neighborhood of the origin in which the map has only a trivial fixed point for small $\varepsilon < 0$ and an extra fixed point $\sqrt{\varepsilon} + ...$ for small $\varepsilon > 0$. The stability of the fixed points is also easily obtained from (4.1). Taking into account that a positive fixed point of the map corresponds to a limit cycle of the system, we can conclude that system (4.2) with any $O(|w|^4)$ terms has a unique (stable) limit cycle bifurcating from the origin and existing for $\varepsilon > 0$. If $s = +1$ an unstable limit cycle appears on $\varepsilon < 0$. Thus, generically the family (2.2) undergoes a Hopf bifurcation, see Fig. 1.

5. BLOW-UP OF THE FOLIATION

To describe the geometry of the foliation of the system, equations (2.2) are blown-up by the complex standard monoidal map (3.3). The blow-up space is equipped with the two charts (V_1, c_1) and (V_2, c_2) which overlap around the equator of the Riemann sphere. The complex equilibrium at zero in (z, w) coordinates splits in two singularities located at $Z = 0$ and $Z = \infty$ on $\mathbb{P}^1$ and those points correspond to $u = +\mathrm{i}$ and $u = -\mathrm{i}$ in the real chart (x, u), see Fig. 3. Inasmuch as the singularity is non-dicritical, the projective line is a common separatrix in the two charts of the blow-up space.

The pullback of (2.2) by the map c_1 yields a system of differential equations in the chart (Z, w) :

$$
(5.1) \qquad \begin{aligned}
\frac{\mathrm{d}Z}{\mathrm{d}t} &= 2\mathrm{i}Z + \sum_{j+k\geq 4} (a_{jk}(\varepsilon) - \overline{a_{k+1,j-1}(\overline{\varepsilon})})Z^j w^{k+j-1},\\
\frac{\mathrm{d}w}{\mathrm{d}t} &= (\varepsilon - \mathrm{i})w + sw^3 Z + \sum_{j+k\geq 4} \overline{a_{jk}(\overline{\varepsilon})} Z^k w^{j+k}.
\end{aligned}
$$

The vector field determined by the right-hand side of this equation will be denoted by $\mathbf{F}_{1,\varepsilon}$ in the sequel.

The pullback of (2.2) by the map c_2 yields a system of differential equations in the chart (W, z) :

$$
(5.2) \qquad \begin{aligned}
\frac{\mathrm{d}W}{\mathrm{d}t} &= -2\mathrm{i}W + \sum_{j+k\geq 4} (\overline{a_{jk}(\overline{\varepsilon})} - a_{k+1,j-1}(\varepsilon))W^j z^{k+j-1},\\
\frac{\mathrm{d}z}{\mathrm{d}t} &= (\varepsilon + \mathrm{i})z + sz^3 W + \sum_{j+k\geq 4} a_{jk}(\varepsilon) W^k z^{j+k}.
\end{aligned}
$$

The vector field determined by this system will be denoted by $\mathbf{F}_{2,\varepsilon}$. These vector fields are generic unfoldings of complex resonant saddle points with the ratio of eigenvalues equal to -2 and $-\frac{1}{2}$ respectively [2]. The equilibria are located exactly at $\pm\mathrm{i}$ on the exceptional divisor.

We now investigate how the vector fields $\mathbf{F}_{1,\varepsilon}$, $\mathbf{F}_{2,\varepsilon}$ in the blow-up are related by the $\mathbb{Z}_2$-equivariance of the vector field in the usual chart. In the complex blow-up space, the real plane embeds as the Möbius strip $\mathfrak{M} = \varrho^*\Sigma^+$. This pullback can be explicitly parametrized in terms of the complex charts. For instance in (Z, w) coordinates the strip $\mathfrak{M} = \{Z = \frac{\overline{w}}{w}\}$, whereas $\mathfrak{M} = \{W = \frac{\overline{z}}{z}\}$ in the other chart. Hence, such a surface can be seen as the embedding $\mathbb{R}^2\backslash\{0\} \hookrightarrow \mathbb{R}^4\backslash\{0\}$

$$
(x, y) \mapsto \left(\frac{x^2 - y^2}{x^2 + y^2}, \frac{2xy}{x^2 + y^2}, x, -y \right).
$$

Indeed, points in polar form $(\mathrm{e}^{\mathrm{i}\theta}, r\mathrm{e}^{-\mathrm{i}\frac{\theta}{2}}) \in \mathbb{R}P^1 \times \mathbb{R}^2$ are in 1-to-1 correspondence with points $(\frac{\overline{w}}{w}, w) \in \mathfrak{M}$ with $\theta \in [0, 2\pi)$. The second component $r\mathrm{e}^{-\mathrm{i}\frac{\theta}{2}}$ corresponds to the direction of a real line L through the origin in the real plane $\mathbb{R}^2$. The first component $\mathrm{e}^{\mathrm{i}\theta}$ gives the point of the unit circle (which is homeomorphic to the exceptional real line $\mathbb{R}P^1 \times \{0\}$) in correspondence with the line L' projecting as L on the real plane $\mathbb{R}^2$, see Fig. 5. (Evidently, the manifold defined by the coordinates $(\mathrm{e}^{\mathrm{i}\theta}, r\mathrm{e}^{-\mathrm{i}\frac{\theta}{2}})$ is non-orientable).

This formulation makes clear that the *real* Möbius strip $\mathfrak{M}$ is invariant under the change of charts: $\varphi(\mathfrak{M}) = \mathfrak{M}$. Indeed, $\varphi\left(\frac{\overline{w}}{w}, w\right) = \left(\frac{w}{\overline{w}}, \overline{w}\right) = \left(\frac{\overline{z}}{z}, z\right)$

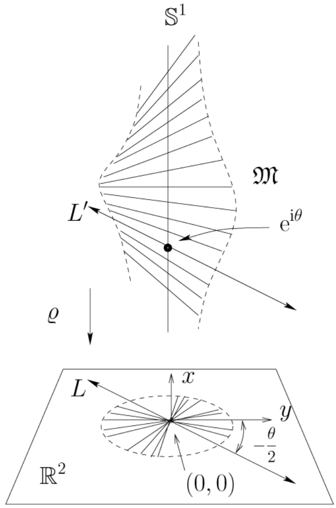

Fig. 5 – The real Möbius strip in complex coordinates.

provided $z = \overline{w}$. Notice that the absolute value of the first coordinate is always 1. The real Möbius strip $\mathfrak{M}$ is then strictly contained in the product $\mathbb{R}P^1 \times \mathbb{R}^2$. The latter is given in complex charts by $\{|Z| = 1\} = \{|W| = 1\}$ within the product $\mathbb{P}^1 \times \mathbb{C}^2$, and by $\{|z| = |w|\}$ in ambient coordinates (z, w). Further, $\mathfrak{M} \subsetneq \mathbb{R}P^1 \times \mathbb{R}^2$ (properly) as real spaces. The real dimension of $\mathbb{R}P^1 \times \mathbb{R}^2$ is 3 and this product is topologically equivalent to the product $\mathbb{S}^1 \times \mathbb{R}^2$ in the blow-up space.

Proposition 5.1. *Denote by τ the involution $(z, w) \mapsto (\overline{z}, \overline{w})$. The $\mathbb{Z}_2$-equivariance* (2.1) *of the family* (2.2) *is equivalent to the symmetric equations*

$$\begin{aligned} \mathbf{F}_{1,\varepsilon} &= \tau \circ \varphi \circ \mathbf{F}_{1,\overline{\varepsilon}} \circ \varphi \circ \tau, \\ \mathbf{F}_{2,\varepsilon} &= \tau \circ \varphi \circ \mathbf{F}_{2,\overline{\varepsilon}} \circ \varphi \circ \tau. \end{aligned} \tag{5.3}$$

Inasmuch as (3.2) *is an involution, this yields* $\mathbf{F}_{1,\varepsilon} = \tau \circ \mathbf{F}_{2,\overline{\varepsilon}} \circ \tau$.

Proof. Inasmuch as $\tau_* = \tau$ and $\sigma_* = \sigma$ (the differentials are computed in $\mathbb{R}^4$), the $\mathbb{Z}_2$-equivariance of the family $\mathbf{F}_\varepsilon$ yields

$$\begin{aligned} \mathbf{F}_{1,\varepsilon} &= (c_1^{-1})_* \mathbf{F}_\varepsilon \circ c_1 \\ &= (c_1^{-1})_* (\sigma \circ \mathbf{F}_{\overline{\varepsilon}} \circ \sigma) \circ c_1 \\ &= c_1^{-1} \circ \sigma \circ \mathbf{F}_{\overline{\varepsilon}} \circ \sigma \circ c_1. \end{aligned}$$

But $c_1^{-1} \circ \sigma = \tau \circ c_2^{-1}$ and $\sigma \circ c_1 = c_1 \circ \varphi \circ \tau$. Thus

$$\begin{aligned} \mathbf{F}_{1,\varepsilon} &= (\tau \circ c_2^{-1})_* \mathbf{F}_{\overline{\varepsilon}} \circ c_1 \circ \varphi \circ \tau \\ &= (\tau \circ \varphi)_* (c_1^{-1})_* \mathbf{F}_{\overline{\varepsilon}} \circ c_1 \circ \varphi \circ \tau \\ &= \tau \circ \varphi \circ \mathbf{F}_{1,\overline{\varepsilon}} \circ \varphi \circ \tau. \end{aligned}$$

In analogous way we prove the other identity and the converse statement. □

Equations (5.3) are referred to as the real character in the blow-up of the family $\mathbf{F}_\varepsilon$.

COROLLARY 5.2. *The $\mathbb{Z}_2$-equivariance is expressed by the invariance of the real Möbius strip $\mathfrak{M}$ under the flows of the systems* (5.1) *and* (5.2) *for real values of the parameter.*

6. COMPLEX HOLONOMIES

In general, the holonomy map between two complex lines through zero in $\mathbb{C}^2$, $\Sigma_a = \{Z = a\}$ and $\Sigma_b = \{Z = \mu_b\}$ is obtained as follows [14]. We lift the radial path defined by the segment between the intersection of the fiber Σ_a with the exceptional divisor (the common separatrix of the foliations of the two charts), and the unit circle $\mathbb{S}^1$. We continue the lifting along $\mathbb{S}^1$ in the counterclockwise direction. Finally, we lift the radial path defined by the segment between the intersection of the fiber Σ_b with the separatrix, and the unit circle $\mathbb{S}^1$.

In particular, the holonomy map sends $\mathfrak{M}$ into itself and it is, hence, *intrinsically real.* In either chart, the counterclockwise direction (with respect to the real equator of the Riemann sphere) will be the *positive* orientation, and the clockwise direction, the *negative* orientation. The direction of the parametrization of the two radial segments depends on whether the modulus of the projection of the fibers on the separatrix, namely $|a|$ and $|b|$, are greater or smaller than 1. In the picture above $|a|, |b| < 1$.

If $a = b = 1$, then the holonomy map coincides with the semimonodromy $\mathcal{Q}_{1,\varepsilon}$ (the semi-monodromy of the field (5.1) for the section Σ in the first chart of the blow-up). Likewise, the holonomy map of the field (5.2) coincides $\mathcal{Q}_{2,\varepsilon}$ provided $a = b = 1$.

COROLLARY 6.1. *The holonomies $\mathcal{Q}_{1,\varepsilon}$ and $\mathcal{Q}_{2,\varepsilon}$ are the inverse of each other.*

Proof. The equator $\mathbb{R}P^1$ is positively parametrized by $(\mathrm{e}^{\mathrm{i}\theta}, 0)$, $\theta \in [0, 2\pi)$ in the first chart of the blow-up. The lifting of this loop in the leaf of the foliation induced by (5.1) through the point $w_0 \in \Sigma$ is given by the trajectory

$\gamma = \{(\mathrm{e}^{\mathrm{i}\theta}, w(\theta)) : \theta \in [0, 2\pi)\}$, where w is the only curve of the field (5.1) satisfying $w(0) = w_0$.

Consider, on the other hand, the lifting of the loop $(\mathrm{e}^{\mathrm{i}\phi}, 0)$, $\phi \in [0, 2\pi)$ in the leaf of the foliation induced by (5.2) starting at the point $w(2\pi) \in \Sigma$ and positively oriented (i.e. oriented in the counter-clockwise direction) in the second chart of the blow-up. Such a lifting is given by $(\mathrm{e}^{\mathrm{i}\phi}, z(\phi))$, where z is the only curve satisfying $z(0) = w(2\pi)$. Since (5.2) is the pullback of (5.1) by the transition (3.2), the trajectory $\gamma^- = \{\varphi(\mathrm{e}^{\mathrm{i}\theta}, w(\theta)) = (\mathrm{e}^{-\mathrm{i}\theta}, \mathrm{e}^{\mathrm{i}\theta} w(\theta)) : \theta \in [0, 2\pi)\}$ is a well-defined lifting in the leaf of the foliation induced by (5.2) passing through the point $(1, w(2\pi))$. However, such a lifting is negatively parametrized (i.e., it is oriented in the clock-wise direction) in the second chart of the blow-up space, because the transition φ reverses the orientation along the equator. Changing the parametrization by $\theta \mapsto 2\pi - \phi$ yields a trajectory $\gamma^+ = \{(\mathrm{e}^{\mathrm{i}\phi}, \mathrm{e}^{-\mathrm{i}\phi} w(2\pi - \phi)) : \phi \in [0, 2\pi)\}$ which starts at $w(2\pi)$. This path is positively oriented in the second chart of the blow-up. Hence, by unicity of solutions in polar coordinates (with the initial condition $w(2\pi)$), we have that $z(\phi) \equiv \mathrm{e}^{-\mathrm{i}\phi} w(2\pi - \phi)$. Thus,

$$\mathcal{Q}_{2,\varepsilon} \circ \mathcal{Q}_{1,\varepsilon}(w_0) = \mathcal{Q}_{2,\varepsilon}(w(2\pi)) = \mathcal{Q}_{2,\varepsilon}(z(0)) = z(2\pi) = w(0) = w_0$$

and the conclusion follows. $\square$

Acknowledgements. The authors are grateful to the anonymous referee for his/her thorough review and highly appreciate the comments and suggestions, which significantly contributed to improving the quality of this publication.

REFERENCES

[1] A. Adler, *Antiholomorphic involutions of analytic families of Abelian varieties.* Trans. Amer. Math. Soc. **254** (1979), 69–94.

[2] W. Arriagada-Silva, *Characterization of the generic unfolding of a weak focus.* J. Differential Equations **253** (2012), 1692–1708.

[3] W. Arriagada-Silva, *Temporally normalizable generic unfoldings of order-1 weak foci.* J. Dyn. Control Syst. **21** (2014), *2*, 239–256.

[4] W. Arriagada and J. Fialho, *Parametric rigidness of germs of analytic unfoldings with a Hopf bifurcation.* Port. Math. **73** (2016), *2*, 156–170.

[5] J. Giné, *Isochronous foci for analytic differential systems.* Internat. J. Bifur. Chaos Appl. Sci. Engrg. **13** (2003), *6*, 1617–1623.

[6] J. Giné and M. Grau, *Characterization of isochronous foci for planar analytic defferential systems.* Proc. Roy. Soc. Edinburgh Sect. A **135** (2005), 985–998.

[7] Y. Il'yashenko, *Nonlinear Stokes phenomena.* Advances in Soviet Mathematics **14**, Amer. Math. Soc., Providence RI, 1993.

[8] Y. Il'yashenko and S. Yakovenko, *Lectures on analytic differential equations.* Grad. Stud. Math. **86**, Amer. Math. Soc., Providence RI, 2008.

[9] H. Jacobowitz, *An introduction to CR structures.* Math. Surveys Monogr. **32**, Amer. Math. Soc., Providence RI, 1990.

[10] Y.A. Kuznetsov, *Elements of applied bifurcation theory.* Appl. Math. Sci. **112**, Springer-Verlag, 1995.

[11] Y. Manin, *Gauge field theory and complex geometry.* A Series of Comprehensive Studies in Mathematics **289**, Springer-Verlag, 1997.

[12] J. Martinet and J.P. Ramis, *Classification analytique des équations différentielles non linéaires résonnantes du premier ordre.* Ann. Sci. Éc. Norm. Supér. (4) **16** (1983), 571–621.

[13] J.K. Moser and S.M. Webster, *Normal forms for real surfaces in $\mathbb{C}^2$ near complex tangents and hyperbolic surface transformations.* Acta Math. **150** (1983), 255–296.

[14] R. Pérez-Marco and J.-C. Yoccoz, *Germes de feuilletages holomorphes à holonomie prescrite.* Astérisque **222** (1994), 345–371.

[15] S. Yakovenko, *A geometric proof of the Bautin theorem.* Amer. Math. Soc. Transl. Ser. 2 **165** (1995), 203–219.

Received 13 August 2017

Khalifa University of Science
and Technology,
Department of Applied Mathematics
and Sciences,
P.O. Box 127788, Abu Dhabi,
United Arab Emirates
waldo.arriagada@ku.ac.ae

Nazarbayev University,
School of Science and Technology,
Department of Mathematics,
53 Kabanbay Batyr Ave.,
Astana 010000 Kazakhstan
piotr.skrzypacz@nu.edu.kz